Shahrood University of Technology

Journal of Hydraulic and Water Engineering (JHWE)

Journal homepage: https://jhwe.shahroodut.ac.ir/

Iranian Hydraulic Association (IHA)

Extraction of Water Surface Changes of Miankale International Wetland using Landsat-8 satellite Images and Fusion of Supervised Classifiers

A. Ghayebi [1,*], E. Zallaghi [2]

[1] Master of Science in Civil Engineering, Expert of Abvaresh Pars Company, Yosefabad, Tehran, Iran.
[2] Ph.D. in Water Resource Engineering, Khuzestan Water and Power Authority (KWPA), Ahwaz, Iran.

Article Info

Article history:

Received: 8 April 2023
Received in revised form: 23 May 2023
Accepted: 15 June 2023
Published online: 17 June 2023

DOI:
10.22044/JHWE.2023.12932.1011

Keywords:
Surface water
Miankale International wetland
Remote sensing
Data fusion
Change detection

Abstract

Among environmental changes, water plays a very vital role in the political, social, and economic issues of countries, which can be used as one of the most practical sources of water supply available to humans and animals. Investigating surface water fluctuations in terms of importance, location, and nature has gained special importance in recent years. Miankale International Wetland with an area of 68,000 hectares in the north of Iran is of special importance. First, by performing radiometric and atmospheric corrections on Landsat-8 satellite images for the years 2013 to 2023 and using the Gram-Schmidt integrator to increase spatial resolution, to extract the NDWI, MNDWI, AWEI, and WI_{2015} indices in order to differentiate the water level. The wetland was treated from non-water. To classify images, supervised classifiers such as maximum likelihood, support vector machine (SVM), and artificial neural network (ANN) were used. Also, to improve the results, the output of the classifiers was merged using the majority voting method. The results of the research showed that the majority voting method was chosen as the most suitable classification method with the highest level of accuracy. In 2023, compared to 2013, the water level of the wetland has decreased from 452.351 km^2 to 298.059 km^2 (34.11%), and the wetland drought has increased from 6.209 km^2 to 160.19 km^2 (more than 2000%). The obtained results can be useful for management decisions to preserve more natural resources in our country.

1. Introduction

We live in a world where water has always been one of its fundamental issues. One of the most important issues related to human society in recent decades is the direct impact of environmental changes on the natural ecosystem, which jeopardizes the ecosystem cycle, and reduces human and animal resources (Alderman et al., 2012). Studying the fluctuations of surface water such as wetlands, lakes, etc. is of particular importance in terms of the importance, location, and nature of these water bodies in recent years. Even today, due to the widespread use of water in drinking, industrial, agricultural, economic, social, security, and political issues, it is obvious that with minimal cost and time savings and without the involvement of expert field mistakes, identifying the characteristics of water areas,

* *Corresponding author:* amirghayebi75@gmail.com, Fax: +98 2333331318, Tel:+989390185061

among these methods, is the use of satellite images in remote sensing technology.

The use of remote sensing is widely used due to its special features such as wide visibility, integration, and the use of different parts of the electromagnetic energy spectrum. They are a very suitable and effective solution to identify and monitor the phenomena and complications of the earth's surface, including surface water, in a short time and in a wide range with the ability to calculate indicators related to hydrological studies (Hester et al., 2008). In the past, various researches have been carried out studies in the field of using remote sensing data to study water resources and investigate the changes in these resources (Harati et al., 2021).

Miankale International Wetland, the first international wetland registered in the list of wetlands of the Ramsar Convention, with an area of more than 68,000 hectares, is one of the important ecosystems and one of the vital areas that has been exposed to drying up in recent years. The serious risk of drought in the Miankale wetland intensified from 2015 onwards, and so far, despite the provision of appropriate solutions, appropriate practical action has not been taken. In this regard, the non-implementation of preventive plans can lead to a bitter fate like that of Urmia Lake for the International Wetland of Miankale. During the last few years, according to experts and researchers, factors such as the receding of the Caspian Sea, the closing of the river to the sea, the decrease in rainfall and the sky's offerings, water scarcity, environmental pollution, the decrease in the volume of water entering the Miankale wetland, and as a result of drought and change The climate has made Miankale wetland dry. Jumaah et al. (2022) Using remote sensing technology, monitored and evaluated the changes in the coastline and water level of Al-Razzah Lake in Iraq from 1989 to 2020. Based on six Landsat-8 and Sentinel-1 satellite images of the study area in 1989, 1999, 2002, 2015, 2019, and 2020, they evaluated the changes and used a supervised SVM[1] algorithm to classify and used water level extraction. The results indicated that with the dramatic change in the lake level, the water area of the lake decreased by 1.84% from 1631.72 km^2 in 1989 to 259.65 km^2 in 2020 (Jumaah et al., 2022).

Keshta et al. (2022) studied the Lake of Burolos, the second-largest lake in the northern part of the Nile Delta in Egypt, in the last 35 years from 1985 to 2020. They used multi-spectral images of Landsat-8 and Sentinel-2 satellites with an average spatial resolution of 10 meters to classify the Borulos Lake area into four main classes, water, marsh, non-vegetated land surfaces (roads, paths, sand sheets, and sand dunes) and used agricultural land. In this classification, the overall accuracy was 96% and the Kappa coefficient was estimated at 0.95. The results showed that this lake had significant losses between 1985 and 2020, and the conversion of wetlands to agricultural land was mainly concentrated in the western and southern parts of the lake, where the area of agricultural land doubled (Keshta et al., 2022).

Helali et al. (2022) using data from Landsat-8 and Modis satellites investigated the changes in the area of Lake Urmia in northwest Iran during 20 years (2000 to 2020). They used indices such as NDVI[2], EVI[3], and NDWI[4] to identify and reveal the water area of Lake Urmia and differentiate between water and non-water. The results showed that NDVI and NDWI were more suitable indicators for monitoring lake water surface changes. Also, the largest area of Lake Urmia was in 2000 and the smallest in 2014 (Helali et al., 2022).

Harati et al. (2021) conducted a research to identify changes in the water area of Urmia Lake and its surrounding vegetation due to annual and long-term variability during the years 2011 to 2016. In their research, by integrating Landsat-7 and Sentinel-2 images, they extracted the NDWI, NDVI, and WI_{2015}[5].

[1] Support Vector Machine
[2] Normalized Difference Vegetation Index
[3] Enhanced Vegetation Index
[4] Normalized Difference Water Index
[5] Water Index

As a result, by integrating the data and increasing the spatial resolution to 15 meters, and using the supervised SVM, NN,[1] and ML[2] algorithms, they classified the images. The results of the study showed that firstly, the level of Urmia Lake has directly and significantly decreased, and on the other hand, changes in the water level of Lake Urmia have led to a general decrease in vegetation in the region (Harati et al., 2021).

According to the research conducted in recent years, we concluded that the use of 15-meter Landsat-8 data and the use of water indicators are emphasized by researchers and help a lot to distinguish water from non-water. The purpose of the research is to extract the surface water of Miankala International Lagoon from 2013 to 2023 and to examine its changes with natural factors such as precipitation, evaporation, temperature, and recent droughts. Also, if policymakers and government environmental organizations ignore the consequences of drought, water crisis, and the continuing downward trend of the water level of the lagoon, risks such as drought, reduction of the cultivated area of agricultural products, loss of natural resources, etc. will threaten the people of the region.

2. Material and Methods

2.1. Study Area

Miankale International Wetland is located in the north of Iran and the south of the Caspian Sea with an area of 68,000 hectares, equivalent to 8.2% of the total area of Mazandaran province. It is located at between the longitudes of 52˚ 24′ 08″ to 54˚ 02′ 02″ east and latitudes ″36˚ 46′ 36″ to 26˚ 36′ 57″ North (Johnson et al., 2018). The geographical location of the studied area is shown in Figure 1.

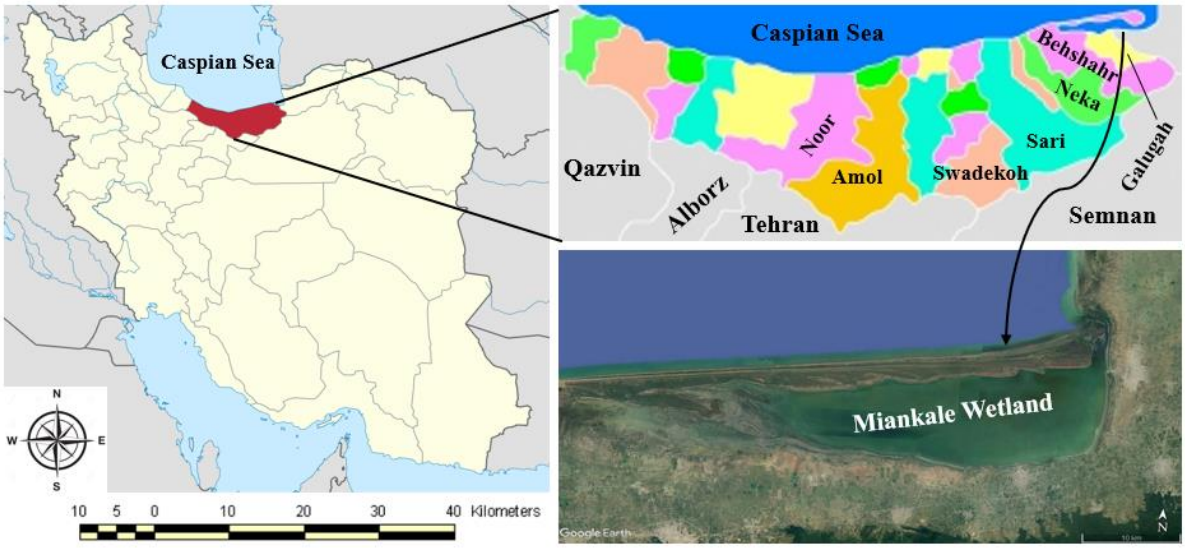

Figure 1. Geographical location of the study area.

2.2 Landsat-8 satellite

The multispectral images of the Landsat-8 satellite have been used to extract the map of the water area of the Miankale Wetland from 2013 to 2023 downloaded from the United States Geological Survey (USGS)[3] website. The specifications of the data used are presented in Table 1.

[1] Neural Network
[2] Maximum Likelihood
[3] https://earthexplorer.usgs.gov

Table 1. Landsat-8 satellite image information.

Satellite	Sensor	Path/Row	Date	Resolution
Landsat-8	OLI	163/34	Mar 27, 2013 Mar 07, 2015 Apr 13, 2017 Mar 02, 2019 Mar 23, 2021 Feb 16, 2023	30m

According to Figure 2, it shows the different stages of the proposed approach to extract surface changes of Miankale International Wetland.

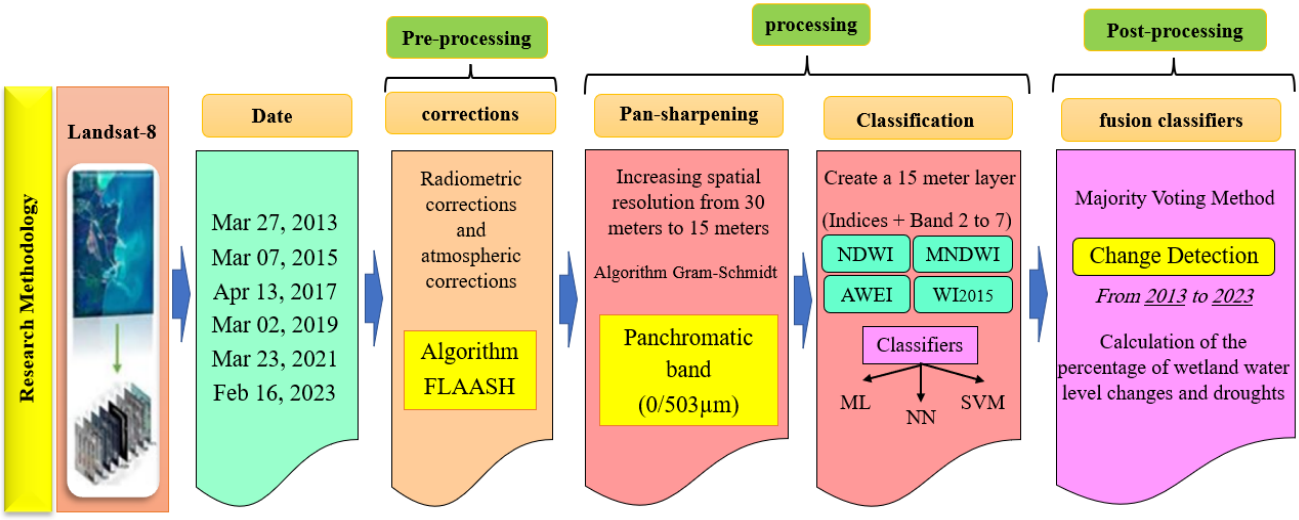

Figure 2. The general research approach for Miankale International Wetland area using Landsat-8 data.

First, Landsat-8 satellite images from 2013 to 2023 have been downloaded from the USGS website. Then, radiometric and atmospheric corrections are performed on the images to achieve the real reflection of the earth in ENVI5.3 software. Then, the radiance values recorded by the Landsat-8 sensor are converted to the real reflection values of the phenomena from the earth's surface using FLAASH[1] algorithms. In pixel-based satellite image fusion, the geometric details of a high-resolution PAN[2] image and spectral information from a low-spatial-resolution MS[3] image are combined to create form a high-spatial-resolution multispectral image. Therefore, with the GS[4] method of pan-sharpening, we upgraded the Landsat-8 images from 30 meters to 15 meters. Finally, in order to distinguish between water and non-water, to reveal the water level of Miankale International Wetland and other complications by extracting four important indices such as the NDWI, MNDWI[5], AWEI,[6]

[1] Fast Line of Sight Atmospheric Analysis of Hypercubes
[2] Panchromatic
[3] Multispectral
[4] Gram-schmidt
[5] Modified Normal Water Difference Index
[6] Automatic Water Extraction Index

and WI_{2015} on 15-meter Landsat-8 images.

2.3. Water Indices

The water indices are the most useful and straightforward methods for enhancing the differences between water and non-water areas, which contain two or more spectral bands of sensors that implement algebraic operations. Table 2 shows the indicators which used in this research.

Table 2. List of indicates used.

Indices	Bands used	Formulas	Author
NDWI	3, 5	$\mathrm{NDWI} = \frac{\mathrm{GREEN} - \mathrm{NIR}}{\mathrm{GREEN} + \mathrm{NIR}}$	(Mc Feeters, 1996)
MNDWI	3, 6	$\mathrm{MNDWI} = \frac{\mathrm{GREEN} - \mathrm{SWIR1}}{\mathrm{GREEN} + \mathrm{SWIR1}}$	(Xu, 2006)
AWEI_nsh	3, 5, 6, 7	$\mathrm{AWEI_{nsh}} = 4(\mathrm{Green} - \mathrm{SWIR1}) - (0.25\mathrm{NIR} + 2.75\mathrm{SWIR2})$	(Feyisa et al., 2014)
WI2015	3, 4, 5, 6, 7	$\mathrm{WI2015} = 1.7204 + 171\mathrm{Green} + 3\mathrm{Red} - 70\mathrm{NIR} - 45\mathrm{SWIR1} - 71\mathrm{SWIR2}$	(Fisher et al., 2016)

2.4. Classification Methods

2.4.1. Maximum Likelihood Classification

The Maximum Likelihood algorithm is one of the most well-known and widely used information classification methods among supervised classification methods. This algorithm is based on probabilities. The probability that a pixel belongs to each class is calculated and assigned to the class with the highest probability (Giardino et al., 2010). In this method, the correlation of the spectral values of different bands is calculated for the sample areas, and the same property is used to relate an unclassified pixel to one of the spectral groups. As a result, each pixel of the image is assigned to the corresponding group after the statistical test and calculation of the probability of their belonging to the spectral groups of the sample (Ahmadpour et al., 2014).

2.4.2. Neural Network Classification

The Neural Network algorithm was first designed by Rosenblatt in 1985. This algorithm is a novel computational system for machine learning, knowledge display, and finally applied knowledge acquisition to maximize the output response of complex systems. A vital element of this idea is the creation of new structures for the information processing system. This approach consists of a large number of highly interconnected processing elements called neurons that work together to solve a problem and transmit information through synapses (Saghafi et al., 2021). For example, by applying the input p to the neuron, it is weighted by multiplying it by the weight w, and it is added with the bias value, which is an adjustable parameter of the neurons, and the result is applied to the transfer function f as input and the final output is obtained. The output of the neuron is calculated as equation 1(Smits et al., 2007).

$$a = f(w * p + b) \quad (1)$$

2.4.3. Support Vector Machine Classification

The original Support Vector Machine algorithm was invented in 1963 by Vapnik. This algorithm is one of the new methods which has good performance compared to older classification methods in recent years (Yves et al., 2001). In the linear classification

of the data, the line that has a higher confidence margin is selected. Considering that SVM is a linear classifier, one can calculate the scalar multiplication, using equation $w^T X = \sum_i w_i x_i$ .This equation is based on the data set $\{(x_i, y_i)\}_{i=1}^n$ where X, is a vector with components x_i and y_i the class defined for the input sample x_i can be defined. Equation 2 shows the general equation of linear classifiers.

$$f(x) = w^T X + b \quad (2)$$

2.4.4. Majority Voting Method

By fusioning classified maps, the weaknesses of different methods can be eliminated and the strengths of each data category can be seen in the final changed map. In this research, the majority voting method was used to integrate the change maps obtained. Voting is a common decision-making fusion method designed to combine the output results of different processors, such as classification results or change maps results. The main idea of this method is that specified results are organized by some special voting rules, such as majority voting and weighted voting rules (Du et al., 2013). Equation 3 describes the algorithm used in this approach.

$$F_{(c,l)} = \frac{(DN_{H(c,l)} - \mu_{H(c,l)})(\sigma_{L(c,l)})}{\sigma_{H(c,l)}} + \mu_{L(c,l)} \quad (3)$$

$F_{(c,l)}$ is the combined image in (c,l) coordinates and also, $DN_{H(c,l)}$ is the image value with high spatial resolution accuracy in (c,l) coordinates. $\mu_{H(c,l)}$ represents the local average value of the image with high spatial resolution at the center of coordinates (c,l). $\mu_{L(c,l)}$ and $\mu_{L(c,l)}$ represent the local average value of the image with high and low spatial resolution accuracy at the center of coordinates (c,l), respectively. $\sigma_{L(c,l)}$ and $\sigma_{H(c,l)}$ show the local average value of the image with high and low spatial resolution accuracy centered is on the coordinates (c,l) (Jawak et al., 2015).

2.4.5. Assessing the accuracy of classifiers

In order to evaluate the accuracy of the results and the classified maps using the Error Matrix, the Overall Accuracy parameters and the Kappa Coefficient were calculated. The overall accuracy is obtained from the ratio of the number of correctly classified pixels to the total number of classified pixels in all classes, calculated by equation 4.

$$O.A. = \frac{1}{N}\sum_{k=1}^{n} a_{kk} \quad (4)$$

In this equation; OA indicates the Overall Accuracy and N is the total number of classified known pixels and the total number of pixels of the main diameter of the error matrix (the total number of correctly classified pixels). The kappa Coefficient calculates the classification accuracy compared to a completely random classification. This coefficient was calculated by using error matrix elements according to equation 5 (Srivastava et al., 2003).

$$k = \frac{N\sum_{i=1}^{r} X_{ii} - \sum_{i=1}^{r}(x_{i+}.x_{+i})}{N^2 - \sum_{i=1}^{r}(x_{i+}.x_{+i})} \quad (5)$$

where r is the sum of the rows or columns in the ambiguity matrix, x_{ii} is the main diameter of the ambiguity matrix, elements x_{i+} and x_{+i} are the sum of the total row i and the total column j, respectively, and N is the total number of pixels (Morss et al., 2005).

3. Results and Discussion

In the proposed approach, the free data of Landsat-8 sensors and the method of data integration were performed to increase the accuracy of spatial resolution. In addition, by adding water indicators, combining them with each other and placing them in a target layer, the accuracy in identifying and extracting

water surface was improved to a very desirable level. Also, the Majority Voting method was used to integrate the data. In the following, the obtained indices were integrated in one layer and finally by sampling the training samples and test samples, classification of the images was done by the desired algorithms. In Table 3, values of Overall Accuracy and Kappa Coefficient for classified 15m Landsat-8 images are shown.

Table 3. Overall Accuracy (OA) and Kappa Coefficient (K) values of Landsat-8 sensor images.

Year	Classifier	OA (%)	K
2013	ML	85.12	0.884
	NN	92.15	0.895
	SVM	95.73	0.941
	MV	98.09	0.992
2015	ML	88.13	0.856
	NN	91.59	0.891
	SVM	96.11	0.952
	MV	99.01	0.994
2017	ML	86.47	0.847
	NN	91.22	0.899
	SVM	96.89	0.955
	MV	99.10	0.996
2019	ML	87.32	0.855
	NN	93.29	0.901
	SVM	97.47	0.958
	MV	98.75	0.998
2021	ML	88.56	0.894
	NN	92.47	0.891
	SVM	97.17	0.950
	MV	98.68	0.989
2023	ML	89.51	0.897
	NN	94.92	0.895
	SVM	98.12	0.984
	MV	98.67	0.978

As shown in table 3 the Majority Voting Method, could predict the water surface of wetland with higher accuracies. The results of merging the classifiers by the majority voting method for the years 2013, 2017, 2019, 2021 and 2023 are shown in Figure 3.

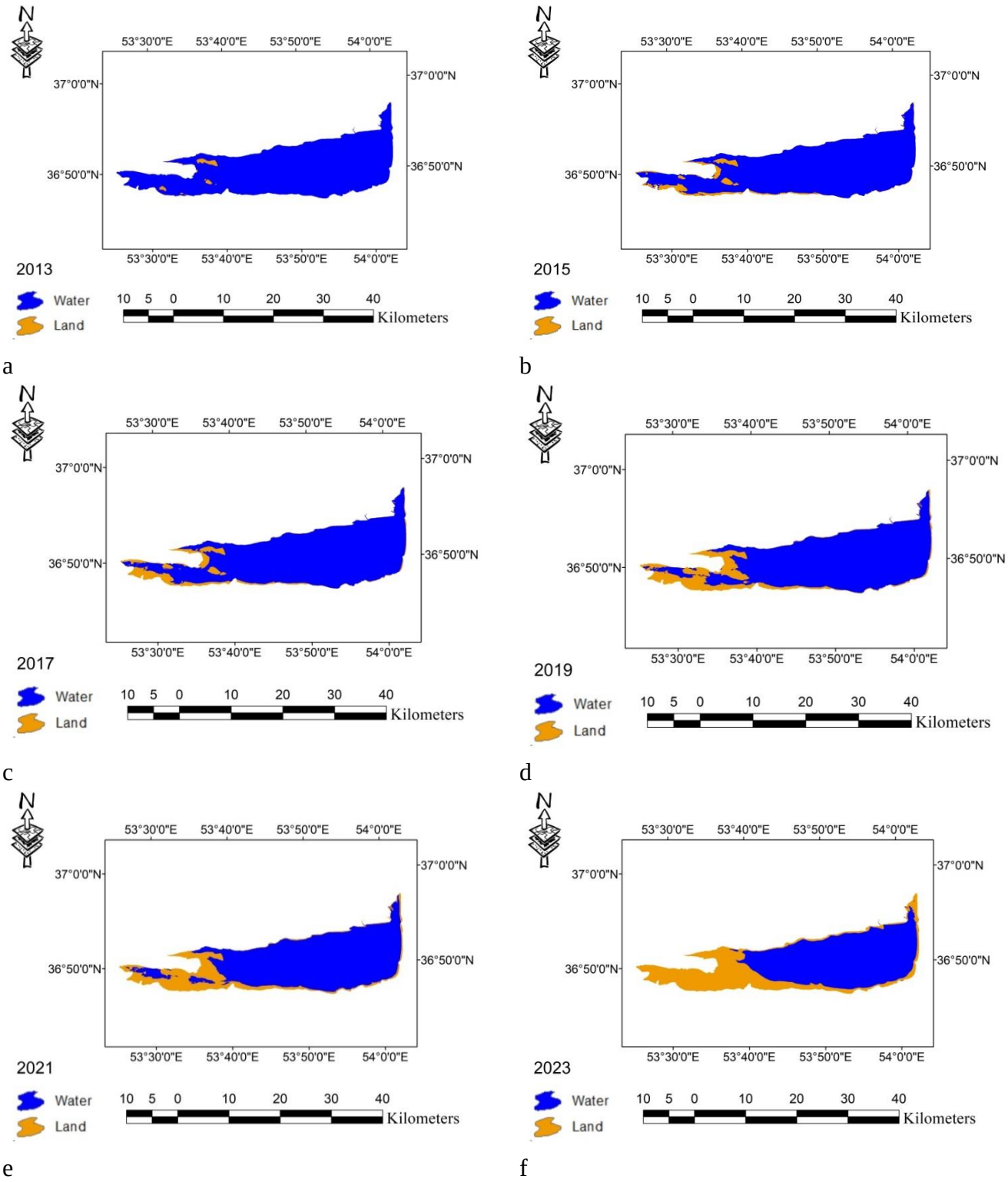

Figure 3. Fusioning the results of classifiers by Majority Voting method. a) Year 2013; b) Year 2015; c) Year 2017; d) Year 2019; e) Year 2021; f) Year 2023.

In table 4, the changes in the estimated area covered by the classes and the percentage of its changes are shown.

Table 4. The amount of area changes and the percentage of class changes.

Years	Class	Area (square kilometers)	(%)Changes
2013-2015	Water	-27.13	-5.997
	Land	27.11	5.597
2015-2017	Water	-2.851	-12.12
	Land	36.420	12.13
2017-2019	Water	-7.883	-32.56
	Land	71.662	32.57
2019-2021	Water	-5.162	-19.65
	Land	25.19	19.66
2021-2023	Water	-62.83	-17.411
	Land	64.326	62.84

Also, by spotting on integrated images and area estimation in ENVI 5.3 software, the graph of the area value of water and land classes is shown in Figures 4 and 5, respectively, from 2013 to 2023.

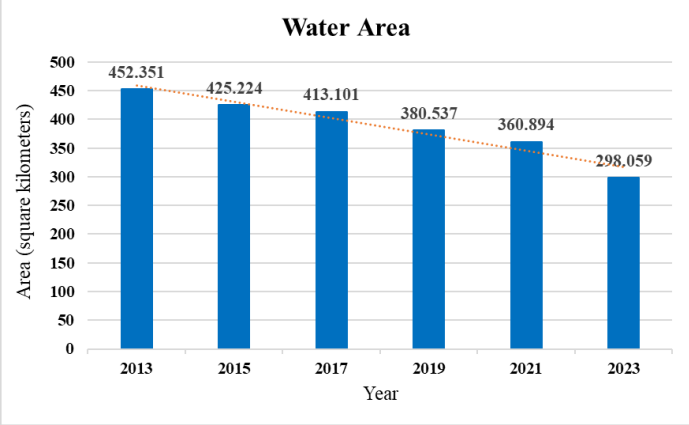

Figure 4. The amount of water area for Miankale Wetland during the years 2013 to 2023.

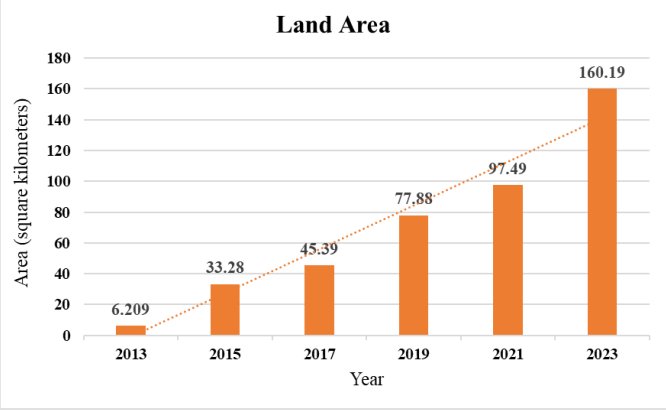

Figure 5. The amount of Land area for Miankale Wetland in the years 2013 to 2023.

The factors affecting wetland drought can be classified into two categories: natural and unnatural. Natural factors such as the Caspian Sea water retreat, the occurrence of drought caused by reducing rainfall, evaporation from water surface due to increasing the temperature and man made factors such as unauthorized constructions, mismanagement of water resources and excessive use of wetland water, drilling of unauthorized wells have played a significant role in wetland drought. Next, the meteorological data of Iran (synoptic stations) such as the monthly average amount of precipitation, temperature and water evaporation of the lagoon were analyzed and the results are shown in figures 6, 7 and 8, respectively.

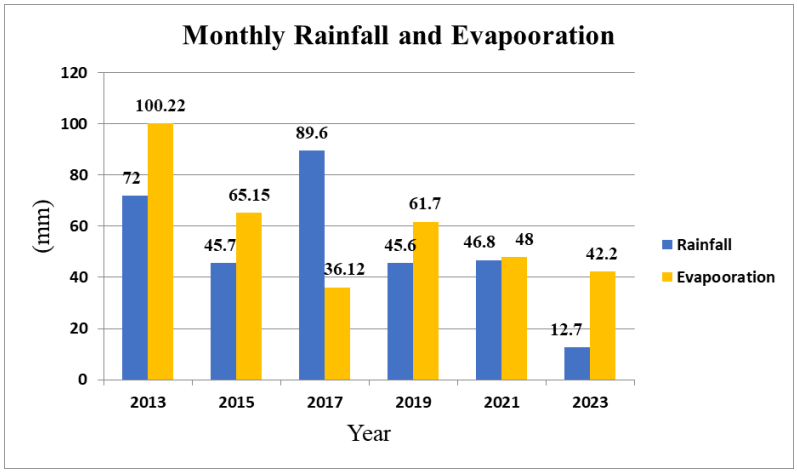

Figure 6. The amount of monthly rainfall and average evaporation for Miankale Wetland in the years 2013 to 2023.

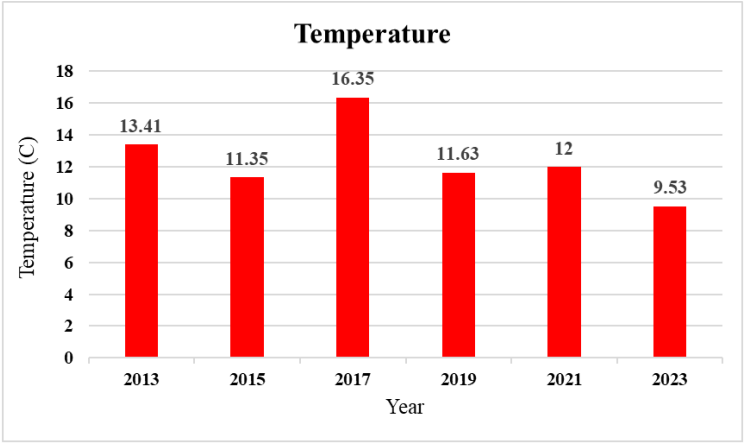

Figure 7. The amount of average Temperature for Miankale Wetland in the years 2013 to 2023.

In this research, the water surface of Miankale International Wetland from 2013 to 2023 was investigated and identified by processing Landsat-8 satellite images; using supervised classifiers and data integration using the majority voting method. The results showed that the majority voting method had higher overall accuracy and kappa coefficients in comparison with other three methods, so this method was chosen to calculate the surface water of the lagoon. Since 2013, this wetland has witnessed many downward surface changes. Recently, the downward trend of the water level of the lagoon in the studied years

had worried the experts and environmentalists, which was faced with the warning of the experts regarding the unfavorable situation of the lagoon. The results indicate that effective factors such as decreasing rainfall and increasing water evaporation on the one hand and neglecting valuable water resources in the country on the other hand have caused the water level of the Wetland between 2013 to 2023 to increase from 351,452 square kilometers to 059,298 square kilometers (34.11 percent) decrease and also increase the amount of wetland drought from 209.6 square kilometers to 19.160 square kilometers (more than 2000 percent). The results of this research can be a way for planners and experts to obtain information about the water level of the Miankale wetland and also to prevent the increase of wetland drought, dust storms and the loss of migratory birds.

References

Ahmadpour A, Solaimani K, Shokri M, Ghorbani J. 2014. Comparison of three common methods in supervised classification of satellite data for vegetation studies. Remote Sensing and Geographic Information System in Natural Resources, 5 (3), 77-89.

Alderman K, Turner L, Tong S. 2012. Floods and human health: a systematic review. Environment international, 47, 37-47. doi:https://doi.org/10.1016/j.envint.2012.06.003.

C. Yves, D. B. Stanislas, B. Marc, M. Fabrice, and L. Gauthier, “RS Data Fusion by Local Mean and Variance Matching Algorithms : their Respective Efficiency in a Complex Urban Context,” no. V, pp. 105–109, 2001.

Du, P., Liu, S., Xia, J., & Zhao, Y. 2013. Information fusion techniques for change detection from multi-temporal remote sensing images. Information Fusion, 14(1), 19-27. doi:https://doi.org/10.1016/j.inffus.2012.05.003

Feyisa G, Meilby H, Fensholt R, Proud S. 2014. Automated Water Extraction Index: A new technique for surface water mapping using Landsat imagery. Remote Sensing of Environment, 140, 23-35. doi:https://doi.org/10.1016/j.rse.2013.08.029.

Giardino C, Bresciani M, Villa P, Martinelli A. 2010. Application of remote sensing in water resource management: the case study of Lake Trasimeno, Italy. Water resources management, 24(14), 3885-3899. doi: 10.1007/s11269-010-9639-3.

Harati, H., Kiadaliri, M., Tavana, A. et al. Urmia Lake dust storms occurrences: investigating the relationships with changes in water zone and land cover in the eastern part using remote sensing and GIS. Environ Monit Assess 193, 70 (2021). https://doi.org/10.1007/s10661-021-08851-3.

Helali, Shahab Asaadi, Teimour Jafarie, Maral Habibi, Saadoun Salimi, Seyed Erfan Momenpour, Salah Shahmoradi, Seyed Asaad Hosseini, Behzad Hessari, Vahideh Saeidi; Drought monitoring and its effects on vegetation and water extent changes using remote sensing data in Urmia Lake watershed, Iran. Journal of Water and Climate Change 1 May 2022; 13 (5): 2107–2128. doi: https://doi.org/10.2166/wcc.2022.460.

Hester, D. B. 2008. Land cover mapping and change detection in urban watersheds using Quickbird high spatial resolution satellite imagery. PhD. dissertation, North Carolina State University, Carolina.

Jawak S, Kulkarni K, Luis A. 2015. A review on extraction of lakes from remotely sensed optical satellite data with a special focus on cryospheric lakes. Advances in Remote Sensing, 4(03), 196. doi:https://doi.org/10.4236/ars.2015.43016.

Johnson B, Tateishi R, Kobayashi T. 2018. Remote sensing of fractional green vegetation cover using spatially-

interpolated endmembers. Remote Sensing, 4(9), 2619-2634. doi:https://doi.org/10.3390/rs4092619.

Jumaah, H. J., Ameen, M. H., Mohamed, G. H., & Ajaj, Q. M. (2022). Monitoring and evaluation Al-Razzaza lake changes in Iraq using GIS and remote sensing technology. The Egyptian Journal of Remote Sensing and Space Science, 25(1), 313-321.

Keshta, A.E.; Riter, J.C.A.; Shaltout, K.H.; Baldwin, A.H.; Kearney, M.; Sharaf El-Din, A.; Eid, E.M. Loss of Coastal Wetlands in Lake Burullus, Egypt: A GIS and Remote-Sensing Study. Sustainability 2022, 14, 4980. https://doi.org/ 10.3390/su14094980.

McFeeters S. 1996. The use of the Normalized Difference Water Index (NDWI) in the delineation of open water features. International journal of remote sensing, 17(7), 1425-1432.doi:https://doi.org/10.1080/01431169608948714.

Morss R, Wilhelmi O, Downton M, Gruntfest E. 2005. Flood risk, uncertainty, and scientific information for decision making: lessons from an interdisciplinary project. Bulletin of the American Meteorological Society, 86(11), 1593-1602. doi:https://doi.org/10.1175/BAMS-86-11-1593.

Saghafi M, Ahmadi A, Bigdeli B. 2021. Sentinel-1 and Sentinel-2 data fusion system for surface water extraction. Journal of Applied Remote Sensing, 15(1), 014521. doi:https://doi.org/10.1117/1.JRS.15.014521.

Smits P, Dellepiane S, Schowengerdt R. 2007. Quality assessment of image classification algorithms for land-cover mapping: a review and a proposal for a cost-based approach. International journal of remote sensing, 20(8), 1461-1486. doi:https://doi.org/10.1080/014311699212560.

Srivastava S, Gupta R. 2003. Monitoring of changes in land use/land cover using multi-sensor satellite data. In Map India Conference.

Xu, H. (2006). A study on information extraction of water body with the modified normalized difference water index (MNDWI). JOURNAL OF REMOTE SENSING-BEIJING-, 9(5), 595.